International Journal of Trend in Scientific Research and Development (IJTSRD)
Volume 7 Issue 1, January-February 2023 Available Online: www.ijtsrd.com e-ISSN: 2456 – 6470

High Efficiency and Thermal Stability: A Downright Response to the Commercialization of Perovskite Solar Cells

Chisom Patrick Mbachu[1,2], Samuel Okechukwu Okozi[1], Eli Danladi[3]

[1]Department of Electrical /Electronic Engineering, Federal University of Technology, Owerri, Nigeria
[2]African Center of Excellence in Future Energies and Electrochemical Systems (ACE-FUELS), Federal University of Technology, Owerri, Nigeria
[3]Department of Physical Sciences, Greenfield University, Kaduna, Nigeria

ABSTRACT

Organo-metal halide perovskites represent a new paradigm for photovoltaics, possessing the propensity to overcome the performance limits of present technologies and achieve low cost and high efficiency and appreciable stability. Recently, efficiencies in excess of 22% has been recorded, but very little is known about their operational characteristics under thermal stress. This paper summarizes the research that focused on the achievements made in the field of perovskite photovoltaics, as well as the principal hurdles to the commercialization of perovskites. In this work, numerical modeling of the planar N-I-P architectural structure (Glass +SnO2:F /TiO2/CH3NH3PbI3/Spiro-OMeTAD/Au) of the Methylammonium Lead Iodide Perovskite Solar Cell was performed for the efficiency improvement of the solar cell. A promising result was achieved with Power Conversion Efficiency (PCE) of 29.31%, Fill Factor (FF) 82.63 %, short-circuit current density (JSC) 23.55 mA/cm2 and open circuit voltage (VOC) 1.51 V. Simulation of the modeled perovskite solar cell was executed using Solar Cell Capacitance Simulator (SCAPS-1D). At higher temperatures, the solar cell's carrier concentration, band gaps, electron and hole mobilities were affected, thus the lower power conversion efficiency. In contrast to the nominal trend where recoded models have their best efficiencies at temperature (measured in Kelvin, K) 300K before consistently decreasing, it was observed that the Power Conversion Efficiency of this model appreciated above 300K hitting a peak efficiency of 29.3445% at 325K, maintained a high efficiency through 355K. The results presented will give a valuable guideline for the feasible fabrication and designing of thermally stable and high power conversion efficiency perovskite solar cells.

How to cite this paper: Chisom Patrick Mbachu | Samuel Okechukwu Okozi | Eli Danladi "High Efficiency and Thermal Stability: A Downright Response to the Commercialization of Perovskite Solar Cells" Published in International Journal of Trend in Scientific Research and Development (ijtsrd), ISSN: 2456-6470, Volume-7 | Issue-1, February 2023, pp.691-703, URL: www.ijtsrd.com/papers/ijtsrd52468.pdf

IJTSRD52468

KEYWORDS: *Perovskite Solar Cell, Commercialization, Thermal Stability, Numerical Modeling*

INTRODUCTION

Photovoltaics have grown at the quickest rate among alternative energy sources in the recent decade. The evolution of photovoltaics from the first generation (mono-crystalline & ploy-crystalline), second generation (amorphous-silicon, CIGS thin film & CDTE thin film) to the third generation/ emerging technologies (concentrated solar cells, polymer-based solar cells, nanocrystal-based solar cells, dye-sensitized solar cells and emphatically, perovskite solar cells) has emphatically been mind blowing. [1]; [2]; [3]; [4]; [5]; [6]; [7]; [8]; [9]; [10].

Perovskite is the scientific name of Calcium Titanate ($CaTiO_3$) mineral, which was originally discovered in 1839 by the German mineralogist Gustav Rose, who named it after a Russian mineralogist- Aleksevich Von Perovski. This explains the unique name, ***PEROVSKI(TES)***. The perovskite or perovskite-related structure can be found in a variety of materials; as a result, it has become a catch-all word for crystals having this structure. Perovskites are minerals that have a similar crystal structure to $CaTiO_3$ but are in a different transition state. The usual stoichiometry of

perovskite crystals is ABX_3, where A is a large organic or inorganic cation ($CH_3NH_3^+$ or $NH_2CH_3NH_2^+$). Cation alloys are being proposed to improve the stability of perovskite absorbers at this point of advanced progress in perovskite materials. B is a divalent inorganic metal cation that is smaller than A; like (Cu^{2+}, Mg^{2+}, Ge^{2+}, Sn^{2+}, Pb^{2+}, Eu^{2+}, Yb^{2+}), where X_3 is a halogen group monovalent anion (such as Cl^-, Br^- and I^-) that can attach to both cations A and B [11]. The atoms are arranged in a cubic lattice as shown in figure 1.

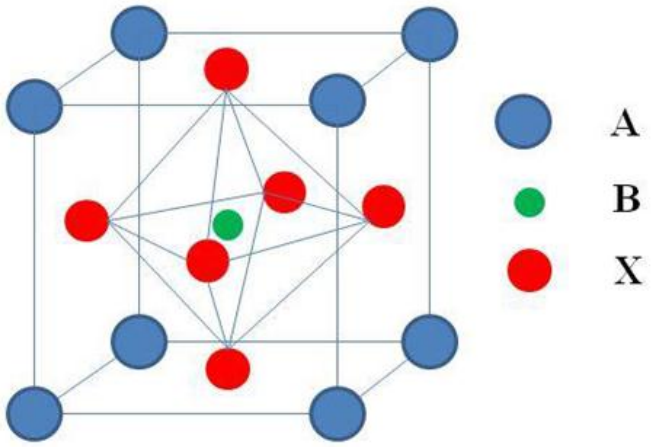

Figure 1: Cubic structure of perovskites [12].

The Organic-Inorganic halide perovskite otherwise called hybrid perovskite is one of the two main categories of perovskite crystal structures which consist of a structure where the octahedral network is composed by an inorganic compound, while the central A-cation is a small organic molecule, usually an amine. Alternatively, this class of compounds can be named organometal trihalide perovskites or metallo-organic perovskites. The general chemical formula for these compounds is ABX_3. The most studied organic groups A at the center of the cage are Methyl Ammonium (MA:$CH_3{-}N^+H_3$) and Formamidinium (FA:$H_3N{-}CH{-}N^+H_3$), with the most common metals in the B-site being Lead and Tin; but other compounds with isovalent metals could also be used; the anion could be a halide chosen between Chlorine, Bromine and Iodine.

1. Literature Review

Perovskite solar cells have been touted as the next big thing in the photovoltaic space and have been intensively studied over time due to their unique properties that include: Having excellent optoelectronic behavior, which enables them function well as the absorber layer for photovoltaic application; Low band gap, which lets more light be absorbed leading to light harvesting from a broad spectrum of incident solar radiation; High charge carrier mobility (hole and electron mobility), which lets the created electrons and holes to move through the material with less resistance; Easy fabricating procedure; Long charge diffusion, etc. In addition, the efficiency of perovskites in recent years have sky-rocketed from meager 2.6% in 2006 [13], to over 22% in 2017 [14] and has more room to improve significantly in the coming years. It is really mind blowing juxtaposing this record with Silicon-based Solar Cells (SSCs) which took more than 40 years for single crystal SSCs to reach the current record of 26%. By and large, this comparison makes perovskite a promising lead in quest for solar cell efficiency improvement. Putting things into perspective, 2017 alone recorded over 3,000 academic journal publications on the subject matter [15]. This goes to show the indefatigable efforts invested by many researchers in perovskite PV and the related areas in a bid to improve device efficiency and stability.

Notable milestones of perovskite solar cells are discussed briefly. Perovskites were first used as light absorbers in solid-state dye-sensitized cells with record efficiency of 2.6% [13]. It further metamorphosed through various stages- quantum dots achieving an increase in efficiency of 6.5% [16], the use of polymers HTM with an efficiency of 9.7% [17]. Persistent efforts by researchers saw the use of polymer HTM + Al_2O_3 scaffold yield an efficiency of 10.9% [18]. Other developmental processes over time made for the significant increase in the efficiency of perovskite solar cells up to 22% [19], [20], [21], [22], [23].

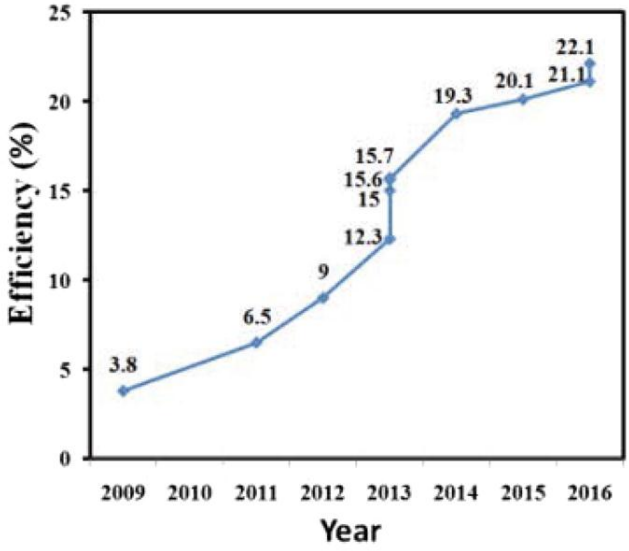

Figure 2: PCE evolution of perovskite solar cells [24]

However in present times, perovskites are solely studied as absorbers in solid state, thin film-like solar cell structures with various cell types spanning a variety of device architectures. Further innovations have given an avenue for developing high performance devices. Such include, but are not

limited to Band gap Engineering, Compositional Engineering and Contact Engineering.

The Band gap Engineering allows for the tunability of perovskites' band gap over a wide range of the solar spectrum. This engineering cuts across various modifications like tandem perovskite cells [25], mixed halides [26] [27]; [28]; [29] [30], hybrid components like the absorber (double or triple absorbers) [31], hybrid charge-transport layers (double HTL or ETL), ETL/HTL-Free cells [32], etc.

Compositional Engineering gives room for the total/partial replacement of constituent materials, be it of inorganic or organic nature. For instance, Compositional engineering of the $MAPbI_3$ perovskite can be achieved by exchanging the organic Methylammonium with Formamidinium (FA); Lead (Pb) metal with Tin (Sn), or Iodine halide with Bromine or Chlorine (Br or Cl). Achieving stable and reproducible high efficiency results is a major concern towards perovskite solar cells' industrialization. Some of the record best perovskite solar cells use mixed organic cations [Methylammonium (MA) and Formamidinium (FA)] and mixed halides [21]. Unfortunately, MA/FA compositions are sensitive to processing conditions because of their intrinsic structural and thermal instability, brought about by impurities domiciled in their films which tend to make them less crystalline. To improve the crystalline property, additional modification has to be introduced. Michael and colleagues introduced small amounts of inorganic cation Cesium (Cs) to a mixed organic cations of Methylammonium and Formamidinium, thus forming a "triple cation" (Cs/MA/FA) configuration which yielded even purer perovskite than the (MA/FA) standalone [22]. This approach is a novel compositional strategy en route to the industrialization of perovskite solar cells with better stabilities and repeatable high efficiencies.

Efforts at making lead-free perovskites by totally replacing lead with other group IVA elements such as Germanium (Ge) and Tin (Sn) have been attempted. Germanium-based perovskites such as $CsGeCl_3$ (Cesium Germanium Chloride) and $MAGeCl_3$ (Methylammonium Germanium Chloride) have be synthesized [33]. More so, a mixed-(Tin & Lead) perovskite has been proven possible and achievable [34].

Contact Engineering takes center stage while studying the properties of the electron and hole collecting electrodes and their interfaces, as they are also critical for improving perovskite device performance. They add to the controlling and modifying of the optoelectronic and structural properties of the absorber[35]; [36]; [37]; [38].

All of these efforts are geared towards significantly improving/increasing the efficiency of perovskite solar cells so that they can compete favorably with the dominant silicon-based solar cells as well as other established thin film solar cells. While the power conversion efficiency of perovskites has rapidly achieved remarkable values, same cannot be said of its stability. Despite numerous strides at overcoming this hurdle, plans of commercialization of perovskites remains bedeviled majorly by thermal instability and low efficiency of the solar cells. Various schools of thought exist as to what the principal encumbrances to the commercialization of perovskites could be.

The first tends to be more/less inclined to business technicalities other than the device technologies. This school of thought has it that one of the most significant hurdles to overcome on the path to commercial success is the issue of raising finance. Scaling up from very promising research results to a technology ready for manufacturing requires an order of magnitude increase in investment. Many venture firms have remained circumspect in investing in PV technology, with the benefit of hind sight into the inrush of PV investments in the mid 2000's, where the likes of TSMC Solar (2015), Helio Volt (2014), Honda Soltec (2013), Nanosolar (2013), Avancis (2013), Solarion (2013), and AQT (2012) either filed for bankruptcy or sold for a fraction of the investment that had attracted.

According to Green et al., (2014), "a key prerequisite for commercialization of perovskite solar-cell technology is a compelling market advantage over incumbent technologies". In terms of cost, the closest commercial technology aside mainstream Silicon-based module that perovskites must compete with is CdTe, (the photovoltaic thin-film technology with the lowest production cost). Aside the draw backs of containing heavy metal, the low material cost of Tellurium (Te) makes it cost effective. Also, fabrication of CdTe is by simple vapour-phase deposition onto FTO-coated glass with a 'glass in' to 'module out' time of 2.5 h [21]. Though perovskite modules could arguably be processed more simply than CdTe modules, the material cost of constituent materials as well as encapsulating materials remains an encumbrance to achieving a lower overall cost. More so, matching the projected efficiencies of CdTe modules in order to gain a competitive advantage will be a workover for perovskite tandem cells, but at a price of increased overall cost. However, with single cells, it

may just be possible for efficiencies of over 20% with extra work, but will contribute to significantly lowering the overall cost.

There is huge reliance on environmentally hazardous heavy metals for high efficiency perovskite solar cells and this is a major obstacle to commercialization, especially with the possibility of large-scale production. However, with lead being at the fore front of for high efficiency perovskite solar cells, its comparison with other lead emission sources such as mining and the manufacture of common products like batteries, plumbing, soldering, and electronic materials, etc., reveals that lead has a very small impact on the overall environmental impact during the manufacturing according to an environmental impact assessment of perovskite solar cells [39]**.** The main concern here is that, as regulation gets more restrictive, technology that relies on hazardous materials may become progressively marginalized. Lead-based perovskite solar cells, on the other hand, may prove to be a problem sink rather than a problem source by allowing for the reuse of lead from other applications, therefore reducing the quantity of lead pollution in the environment. Chen et al., (2014) described the fabrication of lead-based perovskite photovoltaic systems with lead supplies recovered from used vehicle batteries.

Owing to various milestones achieved in the area of perovskites, one might imperatively say that the commercialization of this technology is lurking around the corner. However, thermal instability continues to rear its ugly head; and to address this issue, it is expedient to investigate the effect of temperature effects of the performance of perovskite solar cells. From previous knowledge about the effects of high temperature on materials, we can make deductions on its effect on perovskite solar cells, which of course will not be far-fetched. Conventionally, increased temperature pivotally targets the bonds that hold the atoms of elements together. It continuously and consistently causes a mild vibrational motion that builds up the entropy level in such material, thus causing the weakening and consequent dissociation of the bonds. In the case of perovskite solar cells which are predominantly hybrid in nature and possessing heterojuction qualities, thermal instability is its albatross as high temperatures target the multi-layered junctions, causing them to act like independent materials. As such, high resistance is built up at each layer causing an obstruction to electron and hole movements. This is preceded by high rates of recombination at the interfaces, as well as the bulk of the materials. Photovoltaic cells, like all semiconductor devices, are extremely temperature sensitive. When the temperature of a solar cell rises, the efficiency and power output decreases. This is mostly owing to greater internal carrier recombination rates as a result of higher carrier concentrations. The significance of solar cell module temperature on the behavior of photovoltaic systems cannot be overstated, as it determines the system's efficiency and output energy. The chemical/structural implication is that for materials like $CH_3NH_3PbI_3$, when temperature exceeds the phase transition temperature of the material, it changes from tetragonal to cubic structure in a linear fashion at temperatures between 54˚C and 56˚C [41]; [42].

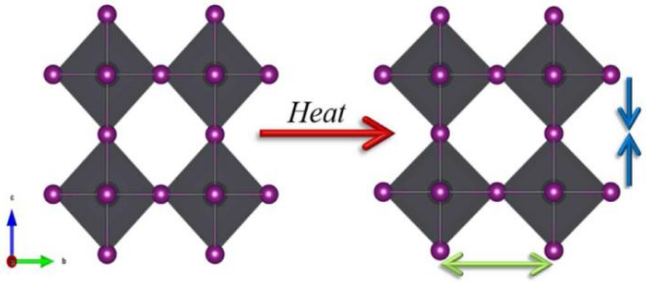

Figure 3: Graphical illustration of the change in the cell structures due to increased temperature [41]

Use of polymers with single-walled Carbon Nanotubes CNTs as a HTL has been reported to increase the thermal stability and retard moisture sensitivity of the perovskite solar cells [43]. Also, sealing of the device has been tried. Even though this technique protects the device against moisture, but it could also cause internal decomposition in the case of an over-sealed situation [44].

The interaction of constituent members of the solar cell with one another at the interface is accounted for by interface engineering. This is crucial to the device's performance since it affects not only exciton generation, dissociation, and recombination, but also the device's deterioration [45]. This further emphasizes the need of interface engineering in achieving high-performance and high-stability PSCs. Interface engineering makes for the control of material behavior by employing different strategies either in material processing or configuration. Tan and co-workers as well as Wang and colleagues have reported various efficiencies by employing different schemes. Efficiencies of 20.1% [46] and 20.3% [47] were respectively reported. Correa-Baena et al. provided some theoretical guidance by investigating in depth the recombination at the different interfaces in a PSC, including the charge-

selective contacts and the effect of grain boundaries [48].

2. Materials and methods

2.1. Modeling of the Perovskite Solar Cell

Modeling is the process of creating a design or representation for the implementation of a physical system using mathematical formulae. Starting a project involving the design of a solar cell without simulation work is a complete waste of time and money. It not only reduces hazards, but also saves time and money. These three (3) major differential equations form the theoretical model of a Perovskite Solar Cell:

A. Poisson's equation.
B. Transport equation, and
C. Continuity equation.

Poisson's equation and continuity equations may be used to explain the performance of a perovskite solar cell in one-dimension. The connection between electric potential and space charges is explained by Poisson's equation. It describes the electric field (E) in delocalized states, traps, and recombination centers, which is a function of the current flowing and the charge. It is written as follows:

$$\frac{\partial^2}{\partial x^2}\Psi(x) = z\frac{q}{\varepsilon}\left[n(x)\text{-}p(x) + N_D^+(x)\text{-}N_A^-(x)\text{-}p_t(x) + n_t(x)\right] \quad (1)$$

The effects of defect density and ionized doping are ignored in a basic model. As a result, the Poisson's equation becomes:

$$\frac{\partial^2}{\partial x^2}\Psi(x) = \frac{q}{\varepsilon}\left[n(x) - p(x)\right] \quad (2)$$

However, when the effects of defect density and ionized doping are taken into account in this model, the Poisson's equation may be recast as:

$$\frac{\partial}{\partial x}\left(\varepsilon\varepsilon_0\frac{\partial\Psi}{\partial x}\right) = -q\left(p - n + N_D^+ - N_A^- + \frac{\rho_{def}}{q}\right) \quad (3)$$

Where;
Ψ is electrostatic potential
ε is permittivity
ε_0 is dielectric constant
q is elementary charge.
P and n are free charge carriers per volume,
N_D^+ and N_A^- are ionized donor and acceptor-like dopants
p_t and n_t are trapped hole and electron density
n and p are density of free electron and hole respectively
ρ_{def} is defect charge density

The conservation of free electrons and free holes in a solar device is defined using continuity equations. The current density of a free electron or hole at any point in the solar cell device must be equal to that at another location in the device at steady state and in the absence of illumination and recombination. These are expressed as

$$-\frac{\partial J_n}{\partial x} - qU_n + qG = q\frac{\partial n}{\partial t} \quad (4a)$$

$$-\frac{\partial J_p}{\partial x} - qU_p + qG = q\frac{\partial p}{\partial t} \quad (4b)$$

Where;
J_n is electron current density
J_p is hole current density
Gs are optical generation rates

Us are recombination rates in the device.
n and p subscripts are for electron and hole respectively
p_t and n_t are trapped hole and electron density

The electron and hole concentrations do not vary with time under a stead state situation, therefore the continuity equations may be reduced to:

$$-\frac{\partial J_n}{\partial x} = -qU_n + qG \quad (5a)$$

$$-\frac{\partial J_p}{\partial x} = -qU_p + qG \quad (5b)$$

The output current of a perovskite solar cell includes diffusion current and drift current caused by electron and hole mobility. These describe the mobility of free electrons and holes in connection to electron and hole current quasi-Fermi level location data. They are given thus:

$$J_n = J_{diffusion} + J_{drift} = -\frac{\mu_n n}{q}\frac{\partial E_{Fn}}{\partial x} = q\mu_n n\frac{\partial\Psi}{\partial x} + qD_n\frac{\partial n}{\partial x} \quad (6a)$$

$$J_p = J_{diffusion} + J_{drift} = +\frac{\mu_p p}{q}\frac{\partial E_{Fp}}{\partial x} = -q\mu_p p\frac{\partial\Psi}{\partial x} + qD_p\frac{\partial p}{\partial x} \quad (6b)$$

Where;
J_n is electron current density
J_p is hole current density
μ_n is electron mobility and
μ_p is hole mobility
n and p are free electrons and holes density, E_{Fn} and E_{Fp} are electron and hole quasi-Fermi level respectively.
D_n and D_p are diffusion coefficient of electrons and holes

All of the charge carriers in the device when it is illuminated will migrate to their associated electrodes, and electrons and holes will strive to

recombine as they move. Three types of recombination processes can be introduced in the bulk of the layer: Defects/Shockley-Read-Hall (SRH), Band-to-Band/Radiative, and Auger recombinations.

Due to intrinsic flaws or impurities in the materials, the Shockley-Read-Hall (SRH) recombination, also known as trap-assisted recombination, occurs. The rate of SRH recombination is calculated as follows:

$$U_{SRH} = \frac{V\sigma_n\sigma_p N_T[np-n_i^2]}{\sigma_p[p+p_1]+\sigma_n[n+n_1]} \quad (7)$$

Where;
σ_n and σ_p are capture cross-sections for electrons and holes,
v is electron thermal velocity,
N_T is number of gap states per volume
n_i and p_i are intrinsic carrier concentrations of electrons and holes,

The phrase "Radiative recombination" or "Band-to-Band recombination" is used to describe the process of photon absorption in reverse. Electrons in the conduction band return to the empty valence band, where they recombine with holes. Radiative recombination rate is expressed as:

$$U_{radiative} = K(np - n_i^2) \quad (8)$$

Where;

$$n_i = N_C\, exp\left(-\frac{E_{gap}}{2v}\right)$$

$$K = \frac{g_{th}^R}{n_i^2}$$

Where;
K = recombination coefficient
v = electron thermal velocity,
N_C = conduction band effective density of states
n_i = intrinsic carrier concentration,
E_{gap} = the actual band gap of the material
g_{th}^R = the number of electrons in conduction band and holes in valence band generated per unit time per unit volume

Auger recombination is a term that describes the recombination of electron and hole pairs when they transition from a high to a low energy state, with the energy transferred to the third carrier. It can be described as follows:

$$U_{Auger} = \left(c_n^A n + c_p^A p\right)(np - n_i^2) \quad (9)$$

Where;
n_i is intrinsic carrier concentration,
c_n^A and c_p^A are constants

Temperature affects the densities of states in the conduction and valence bands, as well as the diffusion coefficient and the thermal velocities of electrons and holes. The influence of temperature on the modeled perovskite solar cell, on the other hand, was given temperature dependency to all other parameters (which is the desired temperature levels).

$$N_c = N_c(T_0)\left[\frac{T}{T_0}\right]^{1.5} \quad (10)$$

$$N_v = N_v(T_0)\left[\frac{T}{T_0}\right]^{1.5} \quad (11)$$

Where;
N_c is conduction band densities of state
N_v is valence band densities of state
T is desired temperature
T_0 = default temperature = 300K

2.2. Numerical Simulation of the Modeled System Using SCAPS-1D

During device simulation, all of the main input parameters must be carefully specified in order to produce a model that acts like an actual equivalent. The simulation software takes the physical parameters of materials as input and converts them into practical or real devices, while expressing the electrical (power conversion efficiency, fill factor, open circuit voltage, and short circuit current) and optical (capacitance and spectral responses/ quantum efficiency) characteristics of the solar cell.

SCAPS-1D examines the layer characteristics and functions in order to improve the solar cell's performance. Layer thickness, electron and hole mobility, electron affinity, band gap, doping density, valence band effective density of state, conduction band effective density of state, electron and hole concentrations, dielectric permittivity, and electron and hole thermal conductivity are the physical parameters used in SCAPS-1D software for numerical analysis.

2.3. Architectural Structure for Model Implementation by SCAPS-1D Modeling of the Perovskite Solar Cell

Figure 4 shows the block design of architecture used in the simulator's simulation of the perovskite solar cell. It depicts a four-layer planar heterojunction structure in its most basic form. Glass + Transparent Conducting Oxide (SnO_2:F), n-type Electron Transportation Layer (TiO_2), Absorber layer/Perovskite Material ($CH_3NH_3PbI_3$), p-type Hole Transportation Layer (Spiro-OMETAD), and Back Contact (Gold) are the device designs that follow the direction of incident light.

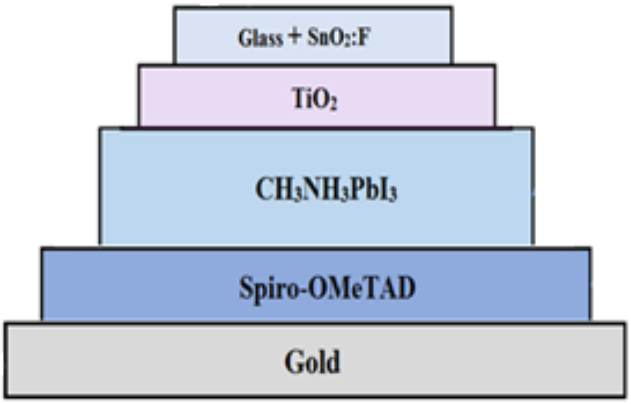

Figure 4: Block diagram of architecture employed in the modeling

On the Solar cell definition panel, the software presents the model of the perovskite solar cell created by SCAPS-1D software, as shown in Figures 5 below. The structure's discretization reveals that red signifies a p-type material and blue denotes an n-type material.

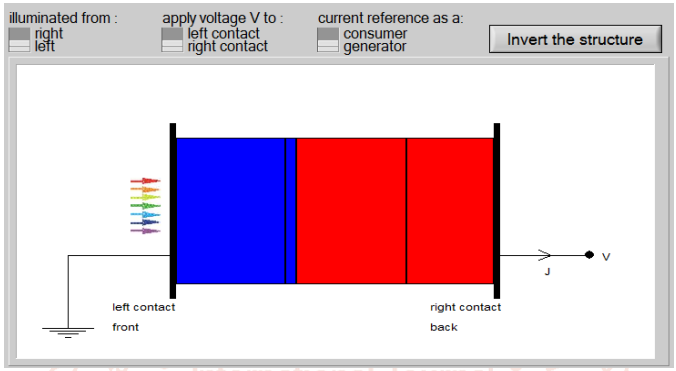

Figure 5: The block diagram as built by SCAPS-1D software

2.4. Baseline Parameters for the Simulation

Table 1 lists the baseline material parameters for each layer employed in this study, which are experimental data from the literature. The donor and acceptor concentrations are denoted by N_D and N_A, respectively. ε_r stands for relative permittivity; Eg stands for bandgap; μ_n and μ_p stand for electron and hole mobilities; N_t stands for defect density; χ denotes electron affinity; CB and VB stand for effective density of states in the conduction band and valence band, respectively. The thermal velocity of electrons and holes, as well as the capture cross section of electrons and holes, are other modeling parameters.

SCAPS have been applied to model the solar cell with charge carrier loss mechanisms in PSCs with Bulk defect densities of $1X10^{15}$ for each layer except for the absorber layer with $2.5X10^{13}$ and interface trap defect densities implemented by Adhikari et al., (2016). In modeling the physical processes, deep insights have been obtained, which helps in determining the characteristic of the solar cell at high temperature.

Table 1: Baseline Parameters for Simulation

Characteristics	SnO_2: F	TiO_2	$CH_3NH_3PbI_3$	Spiro-OMeTAD
Thickness (μm)	0.5	0.05	0.5	0.4
Band gap (eV) Eg	3.5	3.2	1.55	2.91
Electron affinity (eV) χ	4.0	4.0	3.9	2.2
Dielectric permittivity ϵ_r	9.0	100	30	3
CB effective density of states ($1/cm^3$)	$2.20X10^{17}$	$2.0X10^{18}$	$2.2X10^{15}$	$2.5X10^{18}$
VB effective density of states ($1/cm^3$)	$2.20X10^{16}$	$1.0X10^{19}$	$2.2X10^{17}$	$1.8X10^{19}$
Electron thermal velocity (cm/s)	$1X10^7$	$1.0X10^7$	$1.0X10^7$	$1.0X10^7$
Hole thermal velocity (cm/s)	$1X10^7$	$1.0X10^7$	$1.0X10^7$	$1.0X10^7$
Electron mobility (cm^2/Vs)	20	$2.0X10^4$	2	$2.0X10^{-4}$
Hole mobility (cm^2/Vs)	10	$1.0X10^3$	2	$2.0X10^{-4}$
Shallow uniform donor density N_D ($1/cm^3$)	$1X10^{19}$	$5.0X10^{19}$	0	0
Shallow uniform acceptor density N_A ($1/cm^3$)	0	0	$1.0X10^{13}$	$3.0X10^{18}$
Total Defect Density N_T (cm^{-3})	$1X10^{15}$	$1X10^{15}$	$2.5X10^{13}$	$1X10^{15}$

3. RESULTS

In this work, we identified areas of primary loss mechanism due to high temperature to be high bulk radiative recombination and surface recombination at the interfaces/junctions. While the latter is caused by the collection of minority carriers together with the majority at the perovskite/absorbing layer, the ETL and back contact, the former is endemic. Mitigating the effects of surface recombination can be achieved by employing Electron Selective Layer and Hole Selective Layer at the Perovskite layer's junctions. These layers would inhibit the minority charges moving towards the electrodes, thus making the surface recombination have a negligible effect. The introduction of these materials however connotes more materials and increased cost of production. To this effect, it was not considered in this work.

The influence of temperature on the modeled perovskite solar cell was given temperature dependency to all other parameters (which is the desired temperature levels). The temperature (K) was defined as a batch parameter in the Batch Set-up to achieve this. Simulations were run at different temperatures (measured in Kelvin, K), T = 275K - 450K, with a step increase of 25K, to better understand and assess the influence of temperature on the performance of the perovskite solar cell.

3.1. Result of Reference Model

Device features were examined in both dark and light environments. The RED line in figure 6 depicts the dark current, while the BLUE trace depicts the current under illumination. The solar cell acted like a giant flat diode in the absence of illumination (dark), producing a very little current and little or no produced charges. When the solar cell is illuminated, current flows due to charges created by light photons, and the solar cell begins to work. The Blue curve displayed the J-V curve of the simulated model with all of the pre-set parameters, with the following values: maximum power conversion efficiency is 29.31% and FF=82.63%, Jsc= 23.55mA/cm^2, Voc=1.51V.

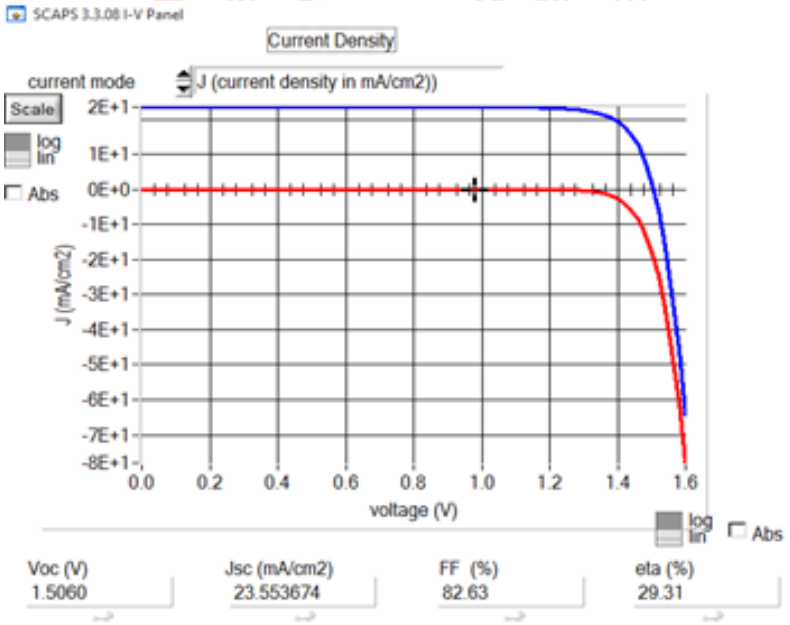

Figure 6: The Dark and Illuminated *J-V* Characteristics of the PSC model

3.2. Quantum Efficiency of the Perovskite Solar Cell Model

The spectral response in Quantum efficiency of a solar cell offers crucial information about the amount of current generated by the cell when irradiated by photons of a specific wavelength, as well as the absorber layer's recombination and diffusion mechanisms. Figure 7 demonstrates that the photon-to-electron conversion ratio, or Quantum Efficiency, is within the wavelength range of 300 to 900 nm at 1 sun, AM1.5G spectrum. This shows the reaction of a typical Methylammonium Lead Iodide ($CH_3NH_3PbI_3$) Perovskite solar cell, which is consistent with previous researches of Eli et al., (2019); Chaudhary & Mehra, (2019); Husainat et al., (2019); Husainat et al., (2020). Below 300 and above 900 nm, light absorption is negligible for this model. The figure shows that between 300 nm and 360 nm, the loss mechanism in quantum efficiency are contributed by SnO_2:F/TiO_2 photon absorption. Thus, higher penetration of light through these layers lowers the quantum efficiency losses. The overall QE of this solar cell indicates that it can absorb photons and effectively convert them into electrons in both Ultraviolet and visible region, which is a very important quality of high performance perovskite solar cells. The optical response of the Perovskite solar cell is demonstrated in figure 7.

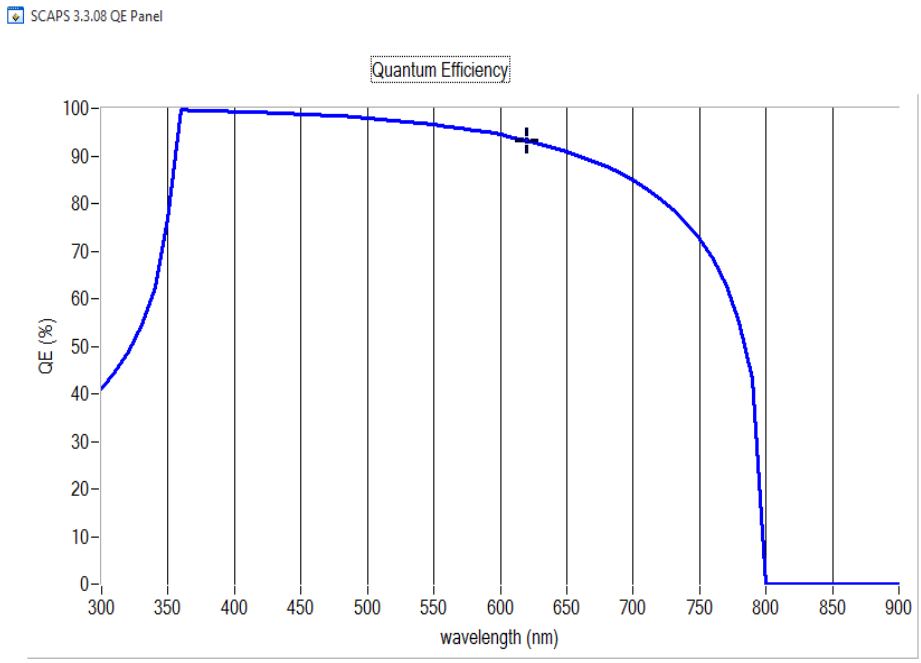

Figure 7: Plot of quantum efficiency with wavelength of PSC model.

3.3. Effect of Temperature on Performance of the Perovskite Solar Cell

Typically, 300K is used as the working temperature in simulation studies and fabrications, where it is considered as the room temperature, although this is not necessarily the case in the open field. Solar cells often operate at temperatures higher than 300K. As a result, the operating temperature domain in this study is set from 275K to 450K with a 25K step increase to better understand the effects of operating temperature on cell performance.

Table 2 Dependence of solar cell performance on the Operating Temperature

T (K)	Jsc (mA/cm^2)	Voc (V)	FF (%)	PCE (%)
275	23.553393	1.4973	82.8975	29.2360
300	23.553674	1.5060	82.6322	29.3119
325	23.553964	1.5102	82.5961	29.3445
350	23.554255	1.5105	82.3365	29.2942
375	23.554491	1.5078	82.1643	29.1803
400	23.554631	1.5027	81.8109	28.9570
425	23.554926	1.4957	81.4477	28.6954
450	23.555224	1.4874	80.9585	28.3637

Figure 8 plots the J-V characteristics of the PSC model with respect to temperature. It was observed that while the J_{SC} consistently increased, V_{OC}, FF and PCE decreased. This gets to show that the solar model performance deteriorated as the operating temperature increased. This is because the solar cell's carrier concentration, band gaps, electron, and hole mobilities are impacted at higher temperatures, resulting in reduced conversion efficiency. Because short circuit current is temperature dependent, V_{OC} decreased as temperature increased. This drop in V_{OC} is mostly due to an increase in short circuit current. This is because the greater operating temperature gives electrons more energy. At greater temperatures, electrons obtain more energy and have a higher level of entropy. They become extremely unstable and are more likely to recombine with the holes before they reach the electrode contacts. These findings are in line with Devi et al., (2018), who found that at high temperatures, electron and hole mobility, carrier concentration, and bandgap will be altered. As a result, the ambient temperature, which has a direct influence on the device temperature, has a significant impact on cell performance, as has been verified by the results in this simulation.

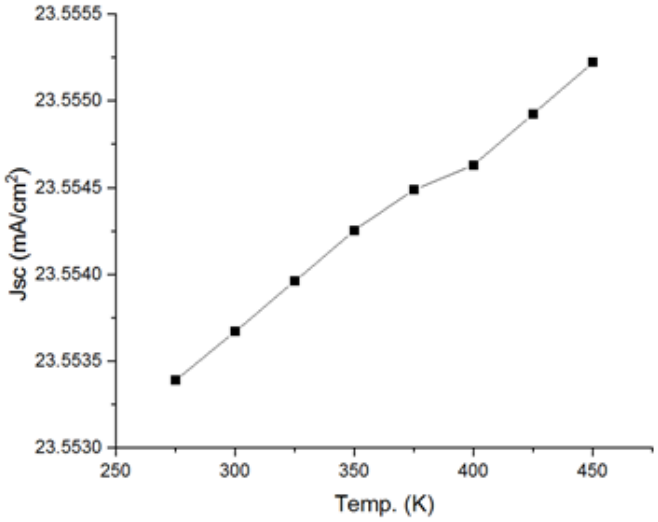

Figure 8: Variation in J_{SC} of PSC model with operating temperature.

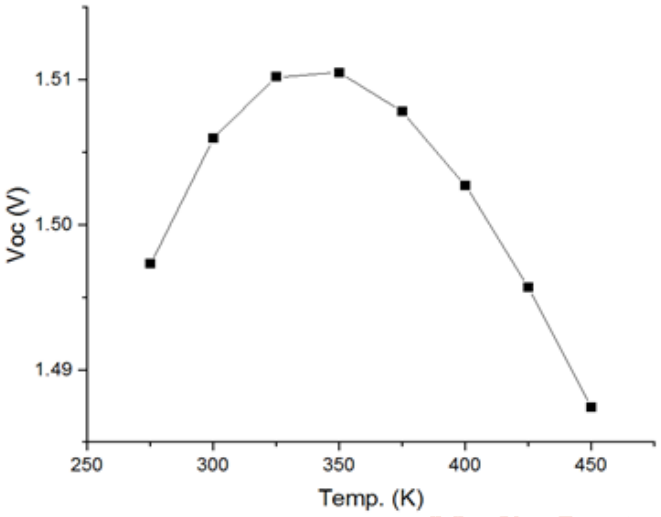

Figure 9: Variation in V_{OC} of PSC model with operating temperature.

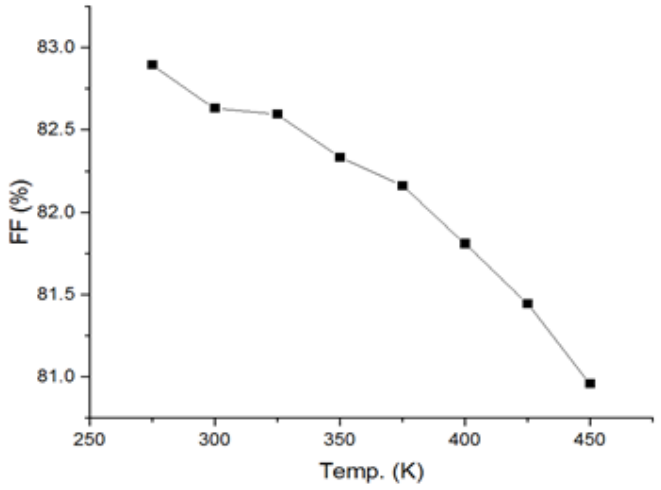

Figure 10: Variation in FF of PSC model with operating temperature.

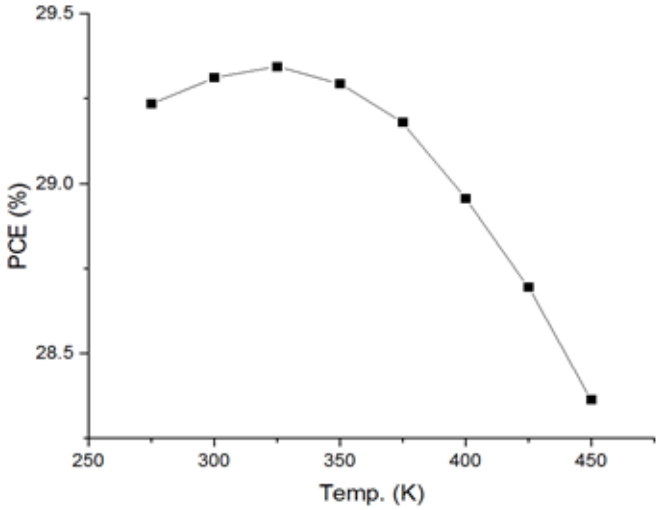

Figure 11: Variation in Efficiency of PSC model with operating temperature.

This model exhibited an excellent character as seen in figure above. In contrast to the nominal trend where the cell efficiency capitulates and takes a downward trend or in the best case scenario remains constant for a very short interval before decreasing, it was observed that V_{OC} and PCE in this model appreciated to a certain point (325K and 355K) above 300K before decreasing. This is a clear indication that this model possesses within it, the propensity to withstand thermal disturbances within these temperature ranges above the standard level of operating temperature. This is a breakthrough in the photovoltaic research space that it is not only thinkable to have stand-alone perovskite solar modules operating efficiently within temperature ranges above 300K and up to 355K, but also feasible and achievable.

4. Conclusion

In this paper, numerical modeling of a lead-based perovskite solar cell was used to investigate the impact of high temperature on the performance of the solar cell. Solar Cell Capacitance Simulator (SCAPS) was used to model, simulate and analyze the device model. Results of the device model gave: a short-circuit current density (Jsc) 23.55 mA/cm^2, an open circuit voltage (Voc) 1.51 V, a Power Conversion Efficiency of 29.31%, and a Fill Factor (FF) of 82.63%. Temperature analysis revealed that V_{OC} and PCE of the model appreciated between 325K and 355K; above 300K standard point before decreasing. This clearly shows that the model has an appreciable ability to withstand thermal disturbances within these high temperature ranges. The findings will be crucial in determining how to fabricate thermally stable and high-efficiency perovskite solar cells.

Data availability

The authors declare that the main data supporting the findings of this study are available within the article. Extra data are available from the corresponding author upon reasonable request.

Acknowledgement

This work is (partially) supported through the Africa Centers of Excellence for Development Impact (ACE Impact) project.

The authors gratefully acknowledge Prof. Marc Burgelman and his team at the Department of Electronics and Information Systems (ELIS), University of Gent, Belgium for providing the SCAPS-1D simulation program.

References

[1] P. Jayakumar, "Solar Energy Resource Assessment Handbook Asian and Pacific Centre for Transfer of Technology," *Renew. Energy Coop. Asia Pacific*, no. September, pp. 1–117, 2009.

[2] K. L. Chopra, P. D. Paulson, and V. Dutta, "Thin-film solar cells: an overview," *Prog. Photovoltaics Res. Appl.*, vol. 12, no. 23, pp. 69–92, 2004, doi:10.1002/pip.541.

[3] S. Sharma, K. K. Jain, and A. Sharma, "Solar Cells : In Research and Applications — A Review," *Mater. Sci. Appl.*, vol. 6, pp. 1145–1155, 2015, doi:10.4236/msa.2015.612113.

[4] A. K. Bansal, "A Review Paper on Development in Material Used in Solar Pannel as Solar Cell Material," *Int. J. Mech. Eng.*, vol. 6, no. 6, pp. 35–41, 2019, doi:10.14445/23488360/ijme-v6i6p107.

[5] A. M. Bagher, M. Mahmoud, A. Vahid, and M. Mohsen, "Types of Solar Cells and Application," vol. 3, no. 5, pp. 94–113, 2015, doi:10.11648/j.ajop.20150305.17.

[6] H. Hoppe and N. S. Sariciftci, "Polymer Solar Cells. Advances in Polymer Science.," *Adv. Polym. Sci.*, vol. 5, no. 1, pp. 1–86, 2007, doi:10.1007/12_2007_121.

[7] P. . Choubey, A. Oudhia, and R. Dewangan, "A review : Solar cell current scenario and future trends," *Recent Res. Sci. Technol.*, vol. 4, no. 8, pp. 99–101, 2012.

[8] A. C. Mayer, S. R. Scully, B. E. Hardin, and M. D. Rowell, Michael W. and McGehee, "Polymer- Based Solar Cells: A Review. Materials Today," *Stanford University, Stanford, CA 94305, USA*, vol. 10, no. 11, pp. 28–33, 2007.

[9] S. Suhaimi, M. M. Shahimin, Z. A. Alahmed, J. Chyský, and A. H. Reshak, "Materials for enhanced dye-sensitized solar cell performance: Electrochemical application," *Int. J. Electrochem. Sci.*, vol. 10, no. 4, pp. 2859–2871, 2015.

[10] U. Mehmood, S. U. Rahman, K. Harrabi, I. A. Hussein, and B. V. S. Reddy, "Recent advances in dye sensitized solar cells," *Adv. Mater. Sci. Eng.*, vol. 2014, 2014, doi:10.1155/2014/974782.

[11] S. Luo and W. A. Daoud, "Recent progress in organic-inorganic halide perovskite solar cells: Mechanisms and material design," *J. Mater. Chem. A*, no. November, pp. 1–19, 2014, doi:10.1039/C4TA04953E.

[12] J. Stenberg, "Perovskite solar cells," Umea University, 2017.

[13] A. Kojima, K. Teshima, Y. Shirai, and T. Miyasaka, "Novel Photoelectrochemical Cell with Mesoscopic Electrodes Sensitized by Lead-halide Compounds.," in *210th ECS Meeting*, 2006, no. 2, p. 397, doi:10.1149/ma2007-02/8/352.

[14] O. K. Simya, A. Mahaboobbatcha, and K. Balachander, "Compositional grading of CZTSSe alloy using exponential and uniform grading laws in SCAPS-ID Simulation," *Superlattices Microstruct.*, vol. 92, pp. 285–293, 2016, doi:10.1016/j.spmi.2016.02.019.

[15] H. J. Snaith, "Present Status and Future Prospects of Perovskite Photovoltaics," *Nat. Mater.*, vol. 17, pp. 372–376, 2018.

[16] J. Im, C. Lee, J. Lee, S. Park, and N. Park, "6.5% efficient perovskite quantum-dot-sensitized solar cell," *Nanoscale*, vol. 3, no. 10, pp. 4088–4093, 2011, doi:10.1039/c1nr10867k.

[17] H. Kim *et al.*, "Lead Iodide Perovskite Sensitized All-Solid-State Submicron Thin Film Mesoscopic Solar Cell with Efficiency Exceeding 9% Hui-Seon," *Sci. Rep.*, vol. 2, no. 591, pp. 1–7, 2012, doi:10.1038/srep00591.

[18] M. M. Lee, J. Teuscher, T. Miyasaka, T. N. Murakami, and H. J. Snaith, "Efficient Hybrid Solar Cells Based on Meso-Superstructured Organometal Halide Perovskites," *Science (80-.).*, vol. 338, no. 6107, pp. 643–647, 2012, doi:10.1126/science.1228604.

[19] O. Malinkiewicz *et al.*, "Perovskite solar cells employing organic charge-transport layers," *Nat. Photonics*, vol. 8, pp. 128–132, 2013, doi:10.1038/nphoton.2013.341.

[20] H. J. Snaith, M. Z. Liu, and M. B. Johnston, "Efficient planar heterojunction perovskite solar cells by vapour deposition," *Nature*, vol. 501, no. 7467, pp. 395–398, 2013, doi:10.1038/nature12509.

[21] M. A. Green, A. Ho-Baillie, and H. J. Snaith, "The emergence of perovskite solar cells," *Nat. Photonics*, vol. 8, no. 7, pp. 506–514, 2014, doi:10.1038/nphoton.2014.134.

[22] M. Saliba *et al.*, "Cesium-containing Triple Cation Perovskite Solar Cells: Improved Stability, Reproducibility and High Efficiency," *Energy Environ. Sci.*, vol. 9, no. 6, pp. 1989–1997, 2016, doi:10.1039/C5EE03874J.

[23] W. S. Yang *et al.*, "Iodide management in formamidinium-lead-halide – based perovskite layers for efficient solar cells," *Science (80-.).*, vol. 356, no. 6345, pp. 1376–1379, 2017.

[24] H. Tang, S. He, and C. Peng, "A Short Progress Report on High-Efficiency Perovskite Solar Cells," *Nanoscale Res. Lett.*, vol. 12, pp. 410–818, 2017, doi:10.1186/s11671-017-2187-5.

[25] A. Rolland *et al.*, "Computational design of high performance hybrid perovskite on silicon tandem solar cells," 2016.

[26] M. Abdi-jalebi *et al.*, "Maximizing and stabilizing luminescence from halide perovskites with potassium passivation," *Nature*, vol. 555, no. 7697, pp. 497–501, 2018, doi:10.1038/nature25989.

[27] S. D. Stranks *et al.*, "Electron-hole diffusion lengths exceeding 1 micrometer in an organometal trihalide perovskite absorber," *Science (80-.).*, vol. 342, no. 6156, pp. 341–344, 2013, doi:10.1126/science.1243982.

[28] J. H. Noh, S. H. Im, J. H. Heo, T. N. Mandal, and S. Il Seok, "Chemical management for colourful, efficient and stable inorganic - organic hybrid nanostructured solar cells," *Nano Lett.*, vol. 13, p. 1764−1769, 2013.

[29] E. Edri *et al.*, "Why lead methylammonium tri-iodide perovskite-based solar cells require a mesoporous electron transporting scaffold (but not necessarily a hole conductor)," *Nano Lett.*, vol. 14, no. 2, pp. 1000–1004, 2014, doi:10.1021/nl404454h.

[30] B. Suarez, V. Gonzalez-Pedro, T. S. Ripolles, R. S. Sanchez, L. Otero, and I. Mora-Sero, "Recombination study of combined halides (Cl, Br, I) perovskite solar cells," *J. Phys. Chem. Lett.*, vol. 5, no. 10, pp. 1628–1635, 2014, doi:10.1021/jz5006797.

[31] I. T. Bello and M. K. Awodele, "Modeling and simulation of CZTS-perovskite sandwiched tandem solar cell," *Turkish J. Phys.*, vol. 48, pp. 321–328, 2018, doi:10.3906/fiz-1801-30.

[32] A. Dymshits, A. Rotem, and L. Etgar, "High voltage in hole conductor free organo metal halide perovskite solar cells," *J. Mater. Chem. A*, vol. 2, no. 48, pp. 20776–20781, 2014, doi:10.1039/c4ta05613b.

[33] T. Baikie *et al.*, "Synthesis and Crystal Chemistry of the Hyrid Perovskite (CH3NH3)PBI3 for Solid-State Sensitized Solar Cell Applications," *J. Mater. Chem. A*, vol. 1, pp. 5628–5641, 2013, doi:10.1039/C3TA10518K.

[34] Y. Ogomi *et al.*, "CH3NH3SnxPb(1-x)I3 Perovskite Solar Cells Covering up to 1060nm," *J. Phys. Chem. Lett.*, vol. 5, no. 6, pp. 1004–1011, 2014, doi:10.1021/jz5002117.

[35] Y. Han *et al.*, "Degradation observations of encapsulated planar CH3NH3PbI3 perovskite solar cells at high temperatures and humidity," *J. Mater. Chem. A*, vol. 3, no. 15, pp. 8139–8147, 2015, doi:10.1039/c5ta00358j.

[36] Y. Kato, L. K. Ono, M. V. Lee, S. Wang, S. R. Raga, and Y. Qi, "Silver Iodide Formation in Methyl Ammonium Lead Iodide Perovskite Solar Cells with Silver Top Electrodes," *Adv. Mater. Interfaces*, vol. 2, no. 13, pp. 2–7, 2015, doi:10.1002/admi.201500195.

[37] L. Fagiolari and F. Bella, "Carbon-based materials for stable, cheaper and large-scale processable perovskite solar cells," *Energy Environ. Sci.*, vol. 12, pp. 3437–3472, 2019, doi:10.1039/c9ee02115a.

[38] A. Husainat, W. Ali, P. Cofie, J. Attia, J. Fuller, and A. Darwish, "Simulation and Analysis Method of Different Back Metals Contact of CH3NH3PbI3 Perovskite Solar Cell Along with Electron Transport Layer

TiO2 Using MBMT-MAPLE/PLD," *Am. J. Opt. Photonics*, vol. 8, no. 1, pp. 6–26, 2020, doi:10.11648/j.ajop.20200801.12.

[39] Z. Song, S. C. Watthage, A. B. Phillips, and M. J. Heben, "Pathways toward high-performance perovskite solar cells : review of recent advances in organo-metal halide perovskites for photovoltaic applications," *J. Photonics Energy*, vol. 6, no. 2, 2016, doi: 10.1117/1.JPE.6.022001.

[40] P. Y. Chen, J. Qi, M. T. Klug, X. Dang, P. T. Hammond, and A. M. Belcher, "Environmentally responsible fabrication of efficient perovskite solar cells from recycled car batteries," *Energy Environ. Sci.*, vol. 7, no. 11, pp. 3659–3665, 2014, doi:10.1039/c4ee00965g.

[41] T. J. Jacobsson, L. J. Schwan, M. Ottosson, A. Hagfeldt, and T. Edvinsson, "Determination of Thermal Expansion Coefficients and Locating the Temperature-Induced Phase Transition in Methylammonium Lead Perovskites Using X-ray Diffraction," *Inorg. Chem.*, vol. 54, no. 22, pp. 10678–10685, 2015, doi:10.1021/acs.inorgchem.5b01481.

[42] A. Poglitsch and D. Weber, "Dynamic disorder in methylammoniumtrihalogenoplumbates (II) observed by millimeter-wave spectroscopy," *J. Chem. Phys.*, vol. 87, no. 11, pp. 6373–6378, 1987, doi:10.1063/1.453467.

[43] S. N. Habisreutinger, T. Leijtens, G. E. Eperon, S. D. Stranks, R. J. Nicholas, and H. J. Snaith, "Carbon Nanotube/Polymer Composites as a Highly Stable Hole Collection Layer in Perovskite Solar Cells," *Nano Lett.*, vol. 14, no. 10, pp. 5561–5568, 2014.

[44] A. K. Baranwal *et al.*, "100C Thermal Stability of Printable Perovskite Solar Cells Using Porous Carbon Counter Electrodes," *ChemSusChem*, vol. 9, pp. 2604–2608, 2016, doi:10.1002/cssc.201600933.

[45] G. Niu, W. Li, J. Li, and L. Wang, "Progress of interface engineering in perovskite solar cells.," *Sci. China Mater.*, vol. 59, no. 9, pp. 728–742, 2016, doi:10.1007/s40843-016-5094-6.

[46] H. Tan *et al.*, "Efficient and stable solution-processed planar perovskite solar cells via contact passivation," *Science (80-.).*, vol. 355, no. 6326, pp. 722–726, 2017, doi:10.1126/science.aai9081.

[47] Q. Wang, Q. Dong, T. Li, A. Gruverman, and J. Huang, "Thin insulating tunneling contacts for efficient and water-resistant perovskite solar cells," *Adv. Mater.*, vol. 28, no. 31, pp. 6734–6739, 2016, doi:10.1002/adma.201600969.

[48] J.-P. Correa-Baena *et al.*, "Identifying and suppressing interfacial recombination to achieve high open-circuit voltage in perovskite solar cells," *Energy Environ. Sci.*, vol. 10, pp. 1207–1212, 2017, doi:10.1039/C7EE00421D.

[49] K. R. Adhikari, S. Gurung, B. K. Bhattarai, and B. M. Soucase, "Comparative study on MAPbI3 based solar cells using different electron transporting materials," *Phys. Status Solidi*, vol. 13, no. 1, pp. 13–17, 2016, doi:10.1002/pssc.201510078.

[50] D. Eli *et al.*, "Simulation and Optimization of Lead-Based Perovskite Solar Cells with Cuprous Oxide as a P-type Inorganic Layer," *J. Niger. Soc. Phys. Sci.*, vol. 1, pp. 72–81, 2019.

[51] S. Chaudhary and R. Mehra, "Synergy of Bis (Sulfanylidene) Tungsten and Spiro-Ometad for an Efficient Perovskite Solar," *Int. J. Eng. Adv. Technol.*, vol. 9, no. 1, pp. 4011–4016, 2019, doi:10.35940/ijeat.A1149.109119.

[52] A. Husainat, W. Ali, P. Cofie, J. Attia, and J. Fuller, "Simulation and Analysis of Methylammonium Lead Iodide (CH3NH3PbI3) Perovskite Solar Cell with Au Contact Using SCAPS 1D Simulator," *Am. J. Opt. Photonics*, vol. 7, no. 2, pp. 33–40, 2019, doi:10.11648/j.ajop.20190702.12.

[53] N. Devi, K. A. Parrey, A. Aziz, and S. Datta, "Numerical simulations of perovskite thin-film solar cells using a CdS hole blocking layer," *J. Vac. Sci. Technol. B*, vol. 36, no. 4, pp. 1–9, 2018, doi:doi:10.1116/1.5026163.